Author/s:
Ashokan, A;Han, J;Hutchison, JA;Mulvaney, P

Title:
Spectroelectrochemistry of CdSe/CdxZn1−xS Nanoplatelets

Date:
2023-01-24

Citation:
Ashokan, A., Han, J., Hutchison, J. A. & Mulvaney, P. (2023). Spectroelectrochemistry of CdSe/CdxZn1−xS Nanoplatelets. ACS Nano, 17 (2), pp.1247-1254. https://doi.org/10.1021/acsnano.2c09298.

Spectroelectrochemistry of CdSe/$Cd_xZn_{1-x}S$ Nanoplatelets

Arun Ashokan, Jiho Han, James A. Hutchison, and Paul Mulvaney*

ARC Centre of Excellence in Exciton Science, School of Chemistry, University of Melbourne, Parkville, Victoria 3010, Australia

E-mail: mulvaney@unimelb.edu.au

Abstract

We report an unexpected enhancement of photoluminescence (PL) in CdSe based core/shell nanoplatelets (NPLs) upon electrochemical hole injection. Moderate hole doping densities induce an enhancement of more than 50% in PL intensity. This is accompanied by a narrowing and blue-shift of the PL spectrum. Simultaneous, time-resolved PL experiments reveal a slower luminescence decay. Such hole induced PL brightening in NPLs is in stark contrast to the usual observation of PL quenching of CdSe based quantum dots following hole injection. We propose that hole injection removes surface traps responsible for the formation of negative trions, thereby blocking non-radiative Auger processes. Continuous photoexcitation causes the enhanced PL intensity to decrease back to its initial level, indicating that photocharging is a key step leading to loss of PL luminescence during normal ageing. Modulating the potential can be used to reversibly enhance or quench the PL, providing a pathway to electro-optical switching.

Keywords: *Photoluminescence, Nanoplatelets, Excitons, Spectroelectrochemistry, Cadmium Selenide*

1. Introduction

The radiative recombination of photogenerated excitons in semiconductor nanocrystals leads to photoluminescence and a key goal is to maximize this PL efficiency. This can be achieved by eliminating the competing non-radiative recombination pathways. Two major non-radiative pathways are Auger recombination and surface trap assisted recombination.[1,2] Auger recombination occurs in semiconductor nanocrystals hosting multicarrier states whereby the photon energy of the exciton excites a third, free carrier which subsequently decays non-radiatively. In nanocrystals where the surfaces are efficiently passivated[3–5] so that surface recombination can be neglected, the Auger pathway limits the overall quantum efficiency. Of course, the trion state itself generally forms following temporary trapping of one photo-generated carrier, presumably in a surface state.[6,7]

Even after such surface passivation by ligands or deposition of a shell layer, the PL can still fluctuate due to the interaction of charge carriers in the band edge and trap states with the environment surrounding the nanocrystals. For example, an oxidative environment has been shown to reduce the luminescence intermittency in spherical CdSe/CdS nanocrystals.[8] Conversely, other researchers have observed that the PL from CdSe/ZnS nanocrystals can be enhanced or reduced in the presence of oxygen.[9,10] Such differences in behaviour can arise due to differences in the synthetic protocols used for making the nanocrystals or to differences in the chemical environment and ligand chemistry.

In order to understand these different behaviours, it is essential to study semiconductor nanocrystals in the presence of different charge carrier populations. One approach to achieving this is by using chemical redox reagents. While chemical oxidants and reductants can be used to fix the redox level in the environment, these agents have a fixed redox potential and chemical byproducts from their reactions may further perturb the system.[11] Hence a more benign method is to use an electrode to provide tunable reducing or oxidising conditions. By adjusting the electrode potential, nanocrystal environments of varying redox potential can be created. So far, such external electrical control of the redox level has mainly focused

on isotropic quantum dots (QDs) with three-dimensional charge carrier confinement.[12–14] Here we study the effects of the redox potential on the optical properties of 1D confined nanoplatelets.

Solution-processed CdSe/$Cd_xZn_{1-x}S$ nanoplatelets (NPLs), where charge carriers are confined in one dimension, have attracted a lot of interest due to their sharp spectral profiles and large oscillator strengths compared to quantum dots.[15]However, NPLs are much more sensitive to the environment. Simple ligand exchange can induce significant shifts in the optical spectra of these materials.[16] Furthermore, the PL of NPLs is very sensitive to oxygen and even low partial oxygen pressures can reduce the luminescence intensity.[17] This is attributed to variations in the charge carrier density of NPLs. Therefore, it is essential to study the influence of varying degrees of carrier density on the spectral features of NPLs. Norris et al. have proposed electrochemical charging as a means to control the charging of nanoplatelets and related spectral broadening.[18] Only a few studies have explored the effects of electrochemical charging on the spectral and electrical properties of nanoplatelets.[17,19–22]

This paper discusses the effect of carrier doping on the optical properties of core/shell NPLs of CdSe. The doping level is controlled electrochemically. A dramatic increase in PL is observed upon increasing the NPL hole density up to a threshold level. Beyond this threshold, the PL starts to quench. Control experiments show that hole transfer from the electrode to NPLs is solely responsible for this behaviour. Based on the simultaneous steady-state and time-resolved photoluminescence measurements during hole injection into NPLs, we propose that the removal of hole traps responsible for efficient negative trion generation is the reason for the PL enhancement.

2.Results

2.1. Hole Injection. Figure 1a shows the photoluminescence spectra of CdSe/$Cd_xZn_{1-x}S$ NPLs with 6 monolayer (ML) thick CdSe NPL cores (referred as 6ML CdSe/$Cd_xZn_{1-x}S$

NPLs) measured during a linear potential sweep from 0 to +2 V at a scan rate of 10 mV/s. From the plot, it is clear that the PL is enhanced during the sweep. The onset of photoluminescence brightening occurs around +0.5 V as shown in Figure 1b. The corresponding voltammogram has a peak around +0.75 V with an onset around +0.5 V (Figure S5b). By the end of the potential sweep, the PL peak intensity increases by 60%. The PL intensity follows a sigmoidal dependence on applied potential and there is a decrease in the FWHM of the PL peak, as shown in Figure 1b,c. The peak emission wavelength, λ_{PL}, also undergoes a small but discernible blue-shift ($\approx$ 1.5 meV) during the potential sweep (Figure 1d). To discharge the 'positively charged' NPLs, the electrode potential can be reset to 0 V. Such a potential step discharges the NPLs faster than when a reverse potential sweep is applied. During discharge, there is quenching of the PL spectra and the final intensity after 200 s is close to, but not identical to, the initial PL intensity (Figure 1e, f). This strongly suggests that the PL changes are a direct result of the presence of added charges. It should be noted that all of these experiments are conducted under continuous laser irradiation and we later show that the quenching happens only under continuous light excitation. Simultaneous PL broadening and a red-shift are observed when discharging the NPLs (Figure 1g, h); however, the recovery is usually incomplete. Note that during the anodic sweep and PL enhancement, the corresponding NPL absorption spectrum remains unchanged. In particular, no bleaching of the exciton band is observed (Figure S1).

PL enhancement upon hole injection is not limited to the 6ML CdSe/$Cd_xZn_{1-x}S$ NPLs. Hole injection into CdSe/$Cd_xZn_{1-x}S$ NPLs with 4 ML thick CdSe NPL cores (referred to as 4ML CdSe/$Cd_xZn_{1-x}S$ NPLs) also results in PL enhancement, irrespective of the aspect ratio (Figure S2). The relationship between PL enhancement and aspect ratio was not studied in detail due to slight differences in the shell thicknesses of these two nanocrystal samples. However, we do find that pure CdS shell coated NPL sample (4ML CdSe/CdS) exhibit similar brightening effects upon hole injection (Figure S3 a), i.e. there is a narrowing and blue-shift of the emission spectrum (Figure S3 b, c). We were also unable to probe the

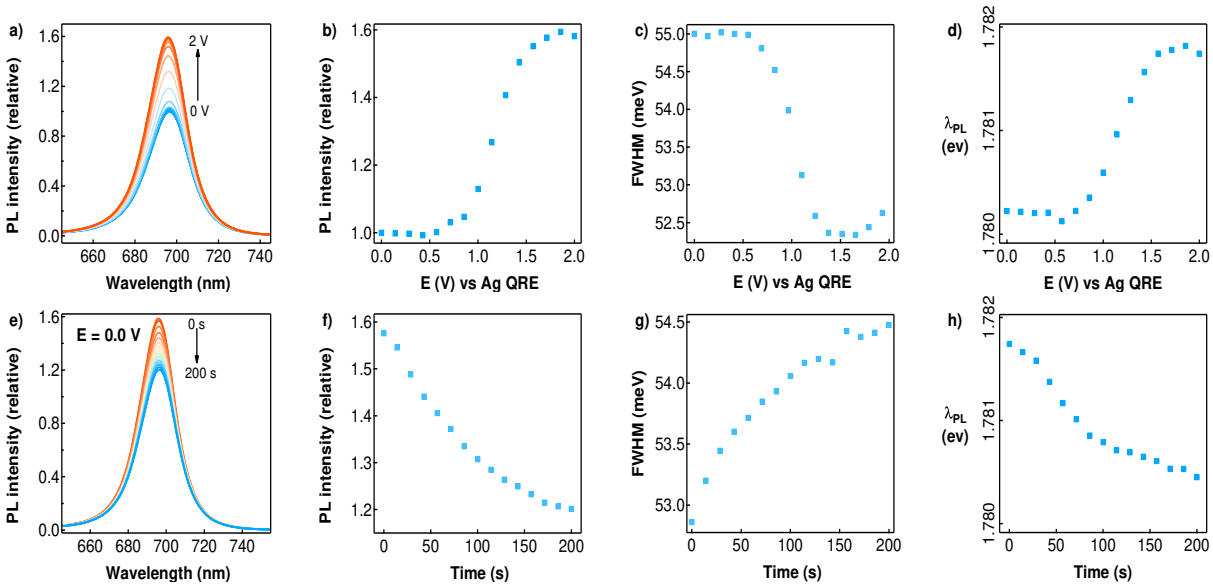

Figure 1: Effect of linear sweep voltammetry on the luminescence of NPLs. (a), (b), (c) and (d): Photoluminescence spectra, PL intensity (λ_{PL}= 696 nm), Full-Width Half Maximum and Peak Emission Wavelength respectively of 6ML CdSe/$Cd_xZn_{1-x}S$ NPLs measured during anodic linear sweep voltammetry from 0 V to 2 V at a scan rate of 10 mV/s. (e), (f), (g) and (h): Photoluminescence spectra, PL intensity, Full-Width Half Maximum and Peak Emission Wavelength respectively of 6ML CdSe/$Cd_xZn_{1-x}S$ NPLs measured after stepping the potential from 2 V back to 0 V. The PL spectra are plotted relative to the PL spectrum measured at open circuit potential ($\approx$ 0 V) and the excitation wavelength was 375 nm. Solution conditions: working and counter electrode = gold, reference electrode = Ag wire, electrolyte was 0.1 M $TBAPF_6$ in N_2 degassed THF).

effects of hole injection on core-NPLs due to aggregation in the polar solvent required for spectroelectrochemistry, as shown in Figure S4.[23] Nevertheless, the above experiments do demonstrate that the PL enhancement observed during hole charging is a general effect for NPLs, irrespective of NPL size, aspect ratio and shell type or thickness.

2.2. Control Experiments. To ensure the effects observed here are due to hole injection, a number of control experiments were carried out. All of the experiments conducted here were carried out in the absence of oxygen and in anhydrous solvents, hence oxygen and water are not responsible for the observed brightening. We note that in a previous study on NPLs, PL brightening in the presence of oxygen was reported.[17] The surface chemistry may also play an important role. Adsorption of surface active ligands such as alkyl amines or halides to NPLs can passivate the nanocrystal surface and this is known to enhance the photoluminescence.[5,24] Decomposition of the quaternary ammonium electrolyte salts used as supporting electrolytes in the electrochemical experiments can also generate such species if the applied potential perturbation is outside the electrochemical window of the electrolyte.[25] However, the absence of any voltammetric peak above the low background current, especially at potentials near the onset of photoluminescence brightening, rules out the possibility of such decomposition (Figure S5a). To further eliminate such possibilities and the effects of any impurities present in the solvent or electrolyte, hole injection experiments were carried out for different electrolyte and solvent combinations. We found that photoluminescence is enhanced in 0.1 M $TBAPF_6$ in acetonitrile-toluene mixtures as well as in 0.1 M $LiClO_4$ in THF (Figure S6). This again rules out the idea that the solvent or electrolyte are responsible for the observed effects. Another possibility is that Ag^+ ions leached from the silver quasi-reference electrode react with the NPLs. This would result in a broad, near-infrared emission which is absent in the conducted experiments.[20] Finally we also checked whether the same effects occur in thin films of NPLs, and to achieve this, the gold mesh working electrode was replaced with an ITO electrode. NPLs were drop-cast onto the electrode directly with no cross-linkers added. PL enhancement was also observed in this case during hole injection

(Figure S7 a, b). Together these experiments rule out the influence of impurities on the observed enhancement and demonstrate that the photoluminescence brightening occurs as a direct result of hole transfer from the electrode to the NPLs.

2.3. Electron Injection. The changes in the optical spectra of NPLs during cathodic sweeps are similar to those reported previously for CdSe based QDs and NPLs.[12,17,19,22,26–28] In the case of electron injection into 6ML CdSe/$Cd_xZn_{1-x}S$ NPLs, there is bleaching of the absorption features during cathodic potential sweeps (Figure 2a). This is normally attributed to filling of the lowest conduction band state. Almost complete bleaching of this transition occurs by the end of cathodic sweeps to -2 V. PL measurements reveal that there is also quenching and broadening of the PL spectra (Figure 2b). Both the absorption and PL spectra show a shift in the peak wavelength during charging. In the case of the heavy hole-conduction band transition, there is no shift during electron injection up to -1.3 V but a clear blue-shift is observed above this potential (Figure S8c). The PL peak wavelength initially starts to red-shift at around -0.7 V and then starts to blue-shift above -1.3 V (Figure S8d).

Figure 2c shows a plot of the changes in absorbance (ΔA) and PL intensity as a function of the cathodic potential sweep. From these data, it is evident that the bleaching and PL quenching both start at $\approx$ -0.7 V. This confirms that there is no significant concentration of electron traps in the core/shell NPLs.[13,26]

2.4. Time-Resolved PL Measurements. Figure 3a shows the PL decay of 6ML CdSe/$Cd_xZn_{1-x}S$ NPLs measured after application of different anodic potential steps with a duration of 600 s. Following each potential step (hole injection) and subsequent lifetime measurements, the potential was stepped back to 0 V and this potential was applied for 800 s to fully discharge the NPLs. The PL decay at a range of potential steps from +0.5 to +2 V was measured; however, only three decays are shown in the graph for clarity. PL decays at all hole-charging potentials and subsequent discharging potentials are shown in the Supporting information (Figure S9). Compared to the PL decay at the open circuit potential (OCP), the PL decay becomes slower at +1.25 V and faster at +2 V. From the log-log plot of PL decay

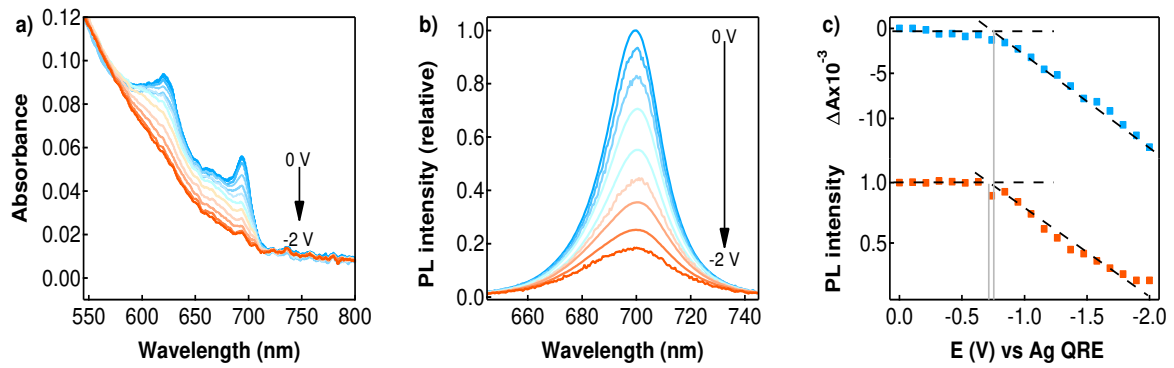

Figure 2: a) Absorption and b) photoluminescence spectra of 6ML CdSe/$Cd_xZn_{1-x}S$ NPLs in 0.1 M $TBAPF_6$ in THF during a cathodic sweep from 0 to -2 V at a scan rate of 10 mV/S. The difference in absorbance, ΔA, (cyan) and PL (orange) of 6ML CdSe/$Cd_xZn_{1-x}S$ NPLs measured during a cathodic potential sweep from 0 to -2 V. The black dotted lines are linear fits to the bleaching and quenching profiles. The onset for the absorption bleach is taken as the conduction band position of the NPLs.

curves with the count normalised at 100 ns plotted in the inset of Figure 3a, it is evident that the amplitude of short lifetime components decreases at +1.25 V and then increases at +2 V with respect to the same lifetimes measured at the OCP. A double exponential function was used to fit the individual decay curves ($I(t) = Y_0 + A_1 \exp\frac{-t}{\tau_1} + A_2 \exp\frac{-t}{\tau_2}$). The average lifetime (τ_{av}) is shown in Figure 3b where $\tau_{av} = \frac{A_1\tau_1 + A_2\tau_2}{A_1 + A_2}$. From Figure 3a and Figure S9, it is clear that the PL decay becomes slower upon hole injection up to +1.25 V. Beyond this potential, the PL decay becomes faster. This is reflected in increases in the average lifetime up to +1.25 V and then decreases beyond that up to +2 V. The inflection point in Figure 3b corresponds to the transition potential, +1.25 V, as the system switches from PL brightening to PL quenching. A similar PL decay response is also observed in the case of CdSe/CdS NPLs (Figure S3d).

It is worth noting that no significant change in PL decay is observed when the NPLs are dispersed in hexane, THF, or when the NPLs are dispersed in the electrolyte solution in the absence of an applied potential (Figure S10). This indicates that the results presented here are independent of the nature of the solvent.

2.5. Effect of light and shape. Increased photoluminescence can also be induced by

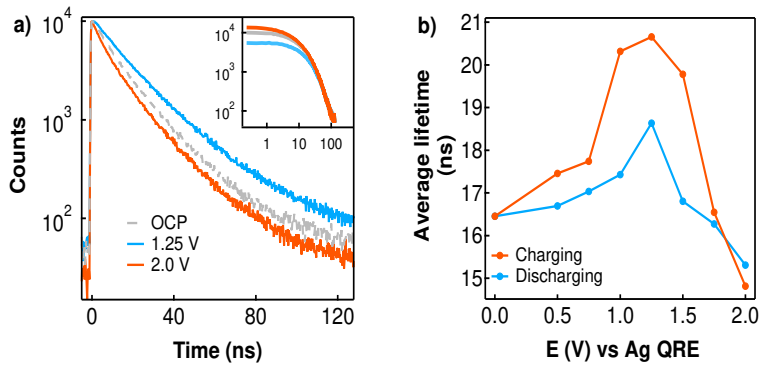

Figure 3: a) PL decay measured at open circuit potential (OCP), 1.25 V, and 2.0 V . Inset shows these PL decay curves normalised at longer time scales. Both counts and time are in log scales. All potentials are measured against Ag QRE. b) Average lifetime calculated from fitting PL decay curves with a double exponential function.

photoexcitation due to various light-activated surface processes including photo-annealing, photoinduced surface rearrangement, and photo-oxidation.[29,30] Hence it was important to determine whether the excitation light had any influence on the PL enhancement and subsequent recovery. To resolve this, the sample PL during an anodic sweep from 0 to +2 V followed by a potential step back to 0 V, was measured under bright and dark conditions. During bright measurements, the PL was measured continuously during laser excitation while for dark measurements the sample was kept in darkness, except for brief illumination during PL measurements i) at the beginning of hole charging, ii) at the end of hole charging and iii) at the end of hole discharging. Figure 4a shows the PL response of 6ML CdSe/$Cd_xZn_{1-x}S$ NPLs during charge-discharge cycles under dark and bright conditions. The light intensity was kept constant during these measurements. Although the PL intensity increased during both light and dark anodic sweeps, the enhancement was much higher for the dark anodic sweep compared to the sweep under illumination. At the end of the anodic potential sweep, the difference in PL intensities between dark and bright measurements was around 30%. This suggested that the light itself was quenching the PL and the net PL enhancement observed during illumination was due to competition between light-induced PL quenching and electrochemically induced brightening. It was also observed that during the discharge potential step back to 0 V, the enhanced PL quenched more slowly in the dark than under illumination

(Figure 4a). Similar results were observed under varying laser intensities (Figure S 11).

To reaffirm the influence of light on PL quenching, the PL enhancement during dark charge/discharge cycles was recorded in the presence and absence of laser illumination. As shown in Figure 4b, there was no significant change in the PL intensity during the 200 seconds of measurement in the dark (The PL was measured only briefly to minimise photo-excitation). After this, the sample was continuously excited with laser light. A clear drop in PL intensity (50%) occurred during this continuous illumination. The very small drop in PL intensity which occurred during the dark conditions may have been due to the brief excitation needed to collect the PL spectra.

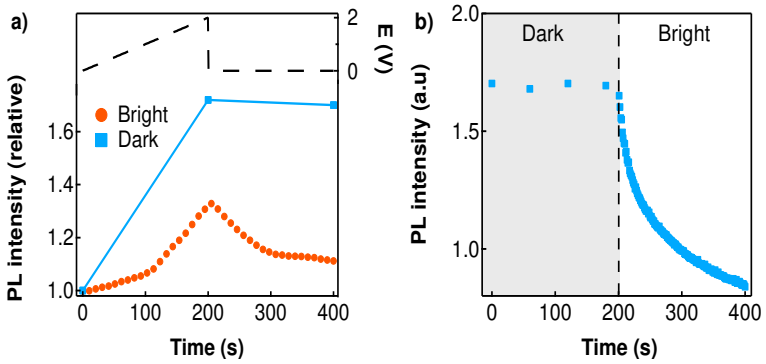

Figure 4: a) Photoluminescence intensity of 6ML CdSe/$Cd_xZn_{1-x}S$ measured during charge-discharge cycles under bright (circle) and dark (square) conditions. The PL intensities are relative to the PL intensity measured at open circuit potential($\approx$ 0 V). The black dotted line shows the potentials applied during the measurements. b) Enhanced PL intensity under dark and bright conditions in the absence of applied potentials.

In order to understand whether the nanocrystal shape plays an important role, charge injection was also carried out on CdSe/$Cd_xZn_{1-x}S$ QDs at similar laser intensities. These QDs had alloyed graded shells which were similar to the graded shells of NPLs. The PL response of these QDs during Fermi level equilibration with the electrode was similar to that found in previous reports and in complete contrast to the behaviour found for these NPLs.[13,31] In particular, we found that injecting QDs with holes quenches the PL (Figure S7c,d) and shortens its lifetime (Figure S12c). The absorption spectra of these QDs remains unchanged during anodic potential sweeps. Discharging of the injected holes leads to only

partial recovery of the PL (Figure S7c,d) as well as its lifetime (Figure S12d).

Even though electron injection into QDs and NPLs results in similar optical responses such as exciton bleaching, PL quenching (Figure S7d), and faster PL decay (Figure S12a), which are indicative of electron charging of CdSe based nanocrystals, a few differences are observed between QDs and NPLs during the discharge following electron injection. The PL intensity recovery in NPLs is higher compared to QDs (Figure S7b, d). But the most significant difference is the slower PL decay measured following the discharge of electron-charged NPLs compared to the PL decay measured for neutral NPLs (Figure S8f), i.e, the PL lifetime is longer after discharge of NPLs than it is when measured initially at OCP. In contrast, for QDs, the PL decay recovers completely after discharge to match PL decay measured initially at the OCP (Figure S12d).

3. Discussion

In contrast to the previous reports on the spectral response of core/shell NPLs upon hole injection,[17,20] the results presented in Figure 1 clearly demonstrate an enhancement in PL during hole injection with simultaneous spectral narrowing and blue-shift (2 meV). Control experiments show that this effect is independent of electrolyte composition, solvent, electrode material, and the aspect ratio of the NPLs. Furthermore, the PL response upon electron injection as shown in Figure 1b, S8 is opposite to that observed during hole injection.

We explain these effects by assuming that a negative trion state is formed in NPLs under photoexcitation through hole trapping and that the luminescence lifetime and QY are therefore reduced due to Auger recombination. This interpretation explains the increase in PL quantum yield, the blue-shift in the PL spectrum since the trion state is at slightly lower energies, and the decrease in PL FWHM is also expected for the exciton state compared to the trion state emission.

In Figure 5, we summarise the effects. Due to ambient lighting excitons are generated

in the NPLs. Holes are trapped on electron-rich surface traps (or on ligands), generating negative trions.[28,32,33] This causes a slow reduction in PL of the NPLs during ageing, due to the onset of Auger recombination. Furthermore, as long as there are significant densities of these surface traps, the PL is low due to this hole trapping.

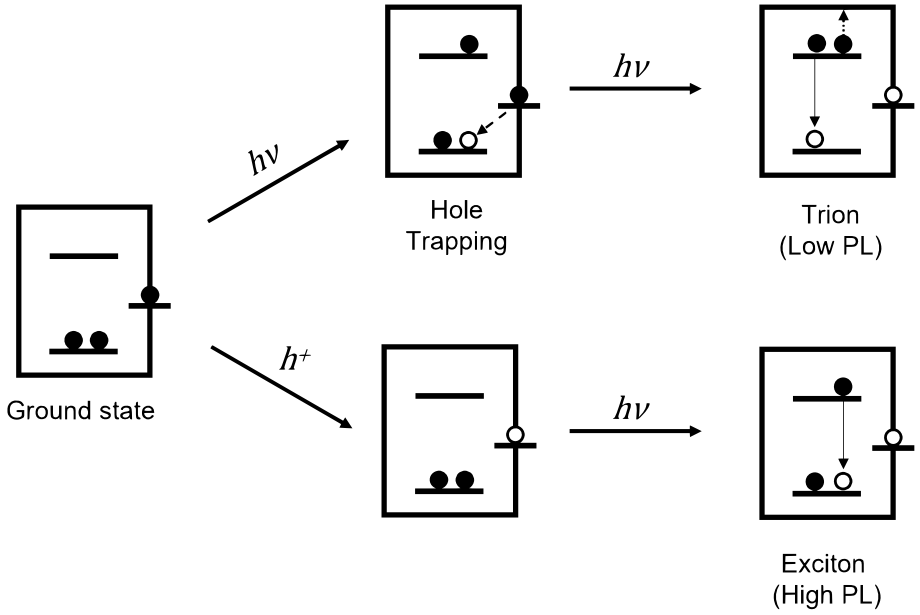

Figure 5: Scheme for the proposed excited state generation during light excitation with and without hole injection.

Hole injection removes electrons in dangling surface states and thereby reduces the rate of non-radiative hole trapping during illumination. Furthermore, the hole injection enables electrons in the conduction band to be removed. Thereafter, NPL emission occurs from the exciton state. All three of these changes in spectral properties turn on at about +1.0 V during the anodic scan and the effect saturates at about +1.5 V. This potential is close to the valence band edge of the NPL. It seems likely that hole injection is into the valence band with its higher density of states, followed by rapid trapping into the surface states. However, it cannot be excluded that holes are injected directly into deep surface states.

Importantly, we do not see bleaching of the exciton transition following hole injection during the potential sweep. Holes in the valence band should contribute to the bleaching as observed for p-type CdTe and CdSe/CdS QDs.[34,35] This shows that holes are not stable in the

valence band and are rapidly trapped. Conversely, the absorption spectra collected during cathodic scans shown in (Figure 2) exhibit bleaching of the exciton transition, indicating that excess electrons are stably stored on these NPLs. These excess electrons result in almost complete PL quenching. The time-resolved PL measured following hole injection also indicates the reduction in negative trion population as the dominant mechanism for PL enhancement. The reduction in the intensity of short lifetime components in the PL decay presented in Figure 3a can be directly related to the reduction of the trion population and indeed, such short decay components have been attributed to trions by other researchers.[36] Our explanation is consistent with previous reports. Negatively charged species have been reported in epitaxially grown 2D II-VI quantum wells.[37–40] In the case of colloidal NPLs, low-temperature PL measurements have confirm the existence of negative trions.[18,28,41–43] Similar studies on CdSe/CdS NPLs have reported the presence of emission features arising from negative trions due to a shake-up process.[43]

Finally, we suggest that the results in Figure 4 can be explained along the same lines. While hole injection leads to PL brightening, the effect is reduced if there is concurrent illumination. Illumination generates large equal numbers of electrons and holes and enables slow re-filling of surface states being emptied by electrochemical hole injection. This will activate the trapping of photogenerated holes and, in turn, leads to the negative trion generation responsible for PL reduction.

The overall PL quantum yield is therefore controlled by the redox potential and the plot in Figure 3b shows there is an optimal environmental redox potential, which maximises NPL luminescence. Increasing the hole injection removes surface electrons which facilitate non-radiative recombination. If hole injection is too intense, positive trions may form and even anodic photocorrosion may eventuate.

4. Conclusion

We have studied the effect of charge carrier injection on the optical properties of NPLs. Interestingly, photoluminescence enhancement is observed during electrochemical hole injection. This is accompanied by a blue-shift, narrowing of the emission spectrum, and slower PL decay. Control experiments exclude the possibility of impurities or the formation of radicals as the origin of the PL enhancement. We conclude that CdSe/$Cd_xZn_{1-x}S$, and CdSe/CdS NPLs have a strong tendency to convert to the trion state upon storage. Ambient light leads to hole trapping on ligands or NPL surface sites and this leads directly to negative trion formation. There is an optimum environmental redox potential, which maximises the PL lifetime by preventing the formation of either positive or negative trion states in the NPLs.

5. Experimental Methods

Synthesis of CdSe nanoplatelets: 4 & 6 ML CdSe NPLs, alloyed CdSe/$Cd_xZn_{1-x}S$, and CdSe/CdS core/shell NPLs were synthesized as reported earlier.[44] CdSe NPLs with different aspect ratios were synthesized by varying the ratio of cadmium acetate precursor.[45] CdSe/$Cd_xZn_{1-x}S$ QDs were synthesized according to procedures reported in the literature.[46] The synthesis yielded NPLs with sharp absorption features and relatively narrow PL (Figure 6 a, b). The core/shell NPLs had a gradient alloyed $Cd_xZn_{1-x}S$ shell which reduced the lattice strain and confined the carriers effectively.[46] There was a considerable red shift in the absorption and emission spectra of the NPLs following the shelling process (See SI Table 1). The luminescence lifetime also increased significantly upon shelling (Figure 6 c, d) (See also SI Table 1). TEM images revealed that the 4 ML NPLs CdSe/$Cd_xZn_{1-x}S$ NPLs were rectangular with an average aspect ratio of 3.36 $\pm$ 0.48 (Figure 6 e) while the 6ML CdSe/$Cd_xZn_{1-x}S$ NPLs were square-shaped with an average aspect ratio of 1.0 $\pm$ 0.1(Figure 6 f).

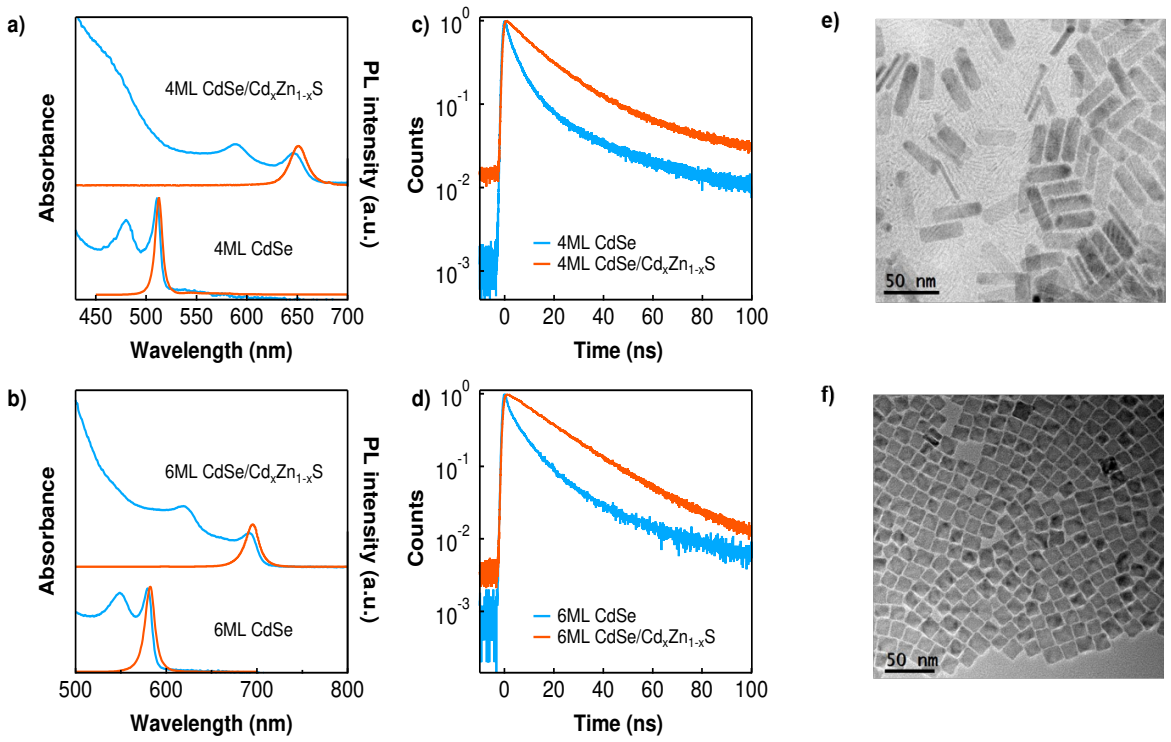

Figure 6: Absorption (cyan) and emission (orange) spectra of CdSe core NPLs & CdSe/Cd_xZn_{1-x} NPLs with core thickness of a) 4 ML & b) 6ML in n-hexane. Spectra of core/shell NPLs are offset along Y axis for clarity. The excitation wavelength was 375 nm. Time-resolved photoluminescence decay of NPLs with c) 4 ML & d) 6ML core thickness. Cyan and orange trace in c) and d) represents the PL decay of core and core/shell NPLs respectively. TEM images of core/shell NPLs of e) 4ML and f) 6ML core thickness. The scale bars in e) and f) are 50 nm.

Instrumentation: Steady-state absorption spectra and fluorescence spectra were collected with an Agilent 8453 UV-visible Spectroscopy System and a Fluorolog Spectrofluorimeter (HORIBA Scientific), respectively. Transmission electron microscopy (TEM) images were collected using a FEI Technai TF20 transmission electron microscope operating at 200 keV. Electrochemical measurements were done using a Metrohm Autolab PGSTAT302. Spectroelectrochemistry (SEC) of NPLs solutions was carried out using a honeycomb electrochemical cell from Pine instruments. All the solvents and electrolytes used for SEC were dried and degassed. Details regarding the assembly of the spectroelectrochemical cell and the drying of solvents can be found elsewhere.[26] The working (WE) and counter electrodes (CE) were gold and the reference electrode (RE) was silver wire. The electrolyte solution

was 0.1 M $TBAPF_6$ in tetrahydrofuran (THF). For control experiments, 0.1 M $TBAPF_6$ in acetonitrile and toluene (1:9) mixture and 0.1 M $LiClO_4$ in THF were used as the electrolyte solution. In case of slight precipitation, the samples were centrifuged to remove the aggregates and the supernatant was used for measurements. Thin-film SEC was carried out using ITO as the WE, a gold coil as CE, and a Ag wire as RE. NPL films were prepared by directly drop-casting the colloid onto the ITO electrode. No crosslinking or spacer layers were used for thin-film SEC. Absorption spectra during the application of potentials were collected using an OceanOptics DH 2000 BAL light source and HR 2000 spectrometer. For emission spectra, the samples were excited using a continuous wave laser source (Shanghai Dream Lasers, λ_{ex} = 375 nm). Due to the enclosed mesh structure of the working electrode, all photoluminescence experiments were made in a collinear configuration. A long-pass filter was used to separate the emission from the excitation beam. A custom setup was used for time-resolved photoluminescence spectroelectrochemistry (TRPL-SEC) (Figure S13). Nanocrystals inside the WE were excited with a pulsed laser (PicoQuant PDL 800-B , λ_{ex} = 470 nm). The repetition rate was 5 MHz. A longpass filter was used to filter out the excitation light from the emission. The emitted photons were then focused onto a fast response avalanche photodiode detector (ID Quantique, ID100). A time-correlated single-photon counting card (PicoQuant, TimeHarp 200) was used to obtain the photoluminescence decay. Overall instrument response function FWHM was ∼200 picoseconds.

Charges were injected into NPLs dispersed in an electrolyte solution by applying a potential to the working electrode (WE). No visible aggregation of NPLs in the electrolyte solutions was observed. Shifting the electrode potentials from the open circuit potential (close to 0 V vs the Ag wire quasi-reference) to negative (cathodic) potentials resulted in electron injection, while a shift to positive (anodic) potentials initiated hole injection. Discharging was achieved by stepping the electrode potential back to 0 V. Both linear sweep voltammetry and potential steps were applied as means to regulate the dynamics of charge injection.

Supporting Information

Interband transition and emission wavelength of core and core/shell NPLs, Cyclic voltammetry of blank solvent, Electron injection into nanoplatelets, Hole charging and discharging in 4ML CdSe/CdS NPL, Hole injection in different electrolytes, Charge injection with ITO electrode, Photoluminescence decay of NPL in different solvents, PL dynamics of QD under charging and discharging, Time resolved spectroelectrochemical set up

Acknowledgement

The authors thank the Australian Research Council (ARC) for support through CE170100026. J.A.H. acknowledges an ARC Future Fellowship award (FT180100295). A.A thank the University of Melbourne for a Melbourne Research Scholarship.

References

(1) Nirmal, M.; Dabbousi, B. O.; Bawendi, M. G.; Macklin, J. J.; Trautman, J. K.; Harris, T. D.; Brus, L. E. Fluorescence intermittency in single cadmium selenide nanocrystals. *Nature* **1996**, *383*, 802–804.

(2) Yuan, G.; Gomez, D. E.; Kirkwood, N.; Boldt, K.; Mulvaney, P. Two mechanisms determine quantum dot blinking. *ACS nano* **2018**, *12*, 3397–3405.

(3) Kirkwood, N.; Monchen, J. O. V.; Crisp, R. W.; Grimaldi, G.; Bergstein, H. A. C.; Du Fossé, I.; Van Der Stam, W.; Infante, I.; Houtepen, A. J. Finding and fixing traps in II–VI and III–V colloidal quantum dots: The importance of Z-type ligand passivation. *Journal of the American Chemical Society* **2018**, *140*, 15712–15723.

(4) Li, J. J.; Wang, Y. A.; Guo, W.; Keay, J. C.; Mishima, T. D.; Johnson, M. B.; Peng, X. Large-Scale Synthesis of Nearly Monodisperse CdSe/CdS Core/Shell Nanocrystals Us-

ing Air-Stable Reagents via Successive Ion Layer Adsorption and Reaction. *Journal of the American Chemical Society* **2003**, *125*, 12567–12575.

(5) Bullen, C.; Mulvaney, P. The Effects of Chemisorption on the Luminescence of CdSe Quantum Dots. *Langmuir* **2006**, *22*, 3007–3013.

(6) Chen, Y.; Vela, J.; Htoon, H.; Casson, J. L.; Werder, D. J.; Bussian, D. A.; Klimov, V. I.; Hollingsworth, J. A. "Giant" Multishell CdSe Nanocrystal Quantum Dots with Suppressed Blinking. *Journal of the American Chemical Society* **2008**, *130*, 5026–5027.

(7) Gong, K.; Kelley, D. F. Surface Charging and Trion Dynamics in CdSe-Based Core/Shell Quantum Dots. *The Journal of Physical Chemistry C* **2015**, *119*, 9637–9645.

(8) Hu, Z.; Liu, S.; Qin, H.; Zhou, J.; Peng, X. Oxygen Stabilizes Photoluminescence of CdSe/CdS Core/Shell Quantum Dots via Deionization. *Journal of the American Chemical Society* **2020**, *142*, 4254–4264.

(9) Koberling, F.; Mews, A.; Basché, T. Oxygen-Induced Blinking of Single CdSe Nanocrystals. *Advanced Materials* **2001**, *13*, 672–676.

(10) Müller, J.; Lupton, J. M.; Rogach, A. L.; Feldmann, J.; Talapin, D. V.; Weller, H. Air-induced fluorescence bursts from single semiconductor nanocrystals. *Applied Physics Letters* **2004**, *85*, 381–383.

(11) Connelly, N. G.; Geiger, W. E. Chemical Redox Agents for Organometallic Chemistry. *Chemical Reviews* **1996**, *96*, 877–910.

(12) Wang, C.; Shim, M.; Guyot-Sionnest, P. Electrochromic nanocrystal quantum dots. *Science* **2001**, *291*, 2390–2392.

(13) Van Der Stam, W.; Grimaldi, G.; Geuchies, J. J.; Gudjonsdottir, S.; Van Uffelen, P. T.; Van Overeem, M.; Brynjarsson, B.; Kirkwood, N.; Houtepen, A. J. Electrochemical

Modulation of the Photophysics of Surface-Localized Trap States in Core/Shell/(Shell) Quantum Dot Films. *Chemistry of Materials* **2019**, *31*, 8484–8493.

(14) Morozov, S.; Pensa, E. L.; Khan, A. H.; Polovitsyn, A.; Cortés, E.; Maier, S. A.; Vezzoli, S.; Moreels, I.; Sapienza, R. Electrical control of single-photon emission in highly charged individual colloidal quantum dots. *Science Advances* **2020**, *6*, eabb1821.

(15) Ithurria, S.; Tessier, M. D.; Mahler, B.; Lobo, R. P. S. M.; Dubertret, B.; Efros, A. L. Colloidal nanoplatelets with two-dimensional electronic structure. *Nature Materials* **2011**, *10*, 936–941.

(16) Diroll, B. T. Ligand-Dependent Tuning of Interband and Intersubband Transitions of Colloidal CdSe Nanoplatelets. *Chemistry of Materials* **2020**, *32*, 5916–5923.

(17) Lorenzon, M.; Christodoulou, S.; Vaccaro, G.; Pedrini, J.; Meinardi, F.; Moreels, I.; Brovelli, S. Reversed oxygen sensing using colloidal quantum wells towards highly emissive photoresponsive varnishes. *Nature communications* **2015**, *6*, 1–9.

(18) Antolinez, F. V.; Rabouw, F. T.; Rossinelli, A. A.; Keitel, R. C.; Cocina, A.; Becker, M. A.; Norris, D. J. Trion Emission Dominates the Low-Temperature Photoluminescence of CdSe Nanoplatelets. *Nano Letters* **2020**, *20*, 5814–5820.

(19) Lhuillier, E.; Ithurria, S.; Descamps-Mandine, A.; Douillard, T.; Castaing, R.; Xu, X. Z.; Taberna, P.-L.; Simon, P.; Aubin, H.; Dubertret, B. Investigating the n-and p-type electrolytic charging of colloidal nanoplatelets. *The Journal of Physical Chemistry C* **2015**, *119*, 21795–21799.

(20) Khan, A. H.; Pinchetti, V.; Tanghe, I.; Dang, Z.; Martín-García, B.; Hens, Z.; Van Thourhout, D.; Geiregat, P.; Brovelli, S.; Moreels, I. Tunable and efficient red to near-infrared photoluminescence by synergistic exploitation of core and surface silver doping of CdSe nanoplatelets. *Chemistry of Materials* **2019**, *31*, 1450–1459.

(21) Geuchies, J. J.; Dijkhuizen, R.; Koel, M.; Grimaldi, G.; du Fossé, I.; Evers, W. H.; Hens, Z.; Houtepen, A. J. Zero-Threshold Optical Gain in Electrochemically Doped Nanoplatelets and the Physics Behind It. *ACS Nano* **2022**, *16*, 18777–18788.

(22) Diroll, B. T.; Chen, M.; Coropceanu, I.; Williams, K. R.; Talapin, D. V.; Guyot-Sionnest, P.; Schaller, R. D. Polarized near-infrared intersubband absorptions in CdSe colloidal quantum wells. *Nature communications* **2019**, *10*, 1–9.

(23) Guzelturk, B.; Erdem, O.; Olutas, M.; Kelestemur, Y.; Demir, H. V. Stacking in Colloidal Nanoplatelets: Tuning Excitonic Properties. *ACS Nano* **2014**, *8*, 12524–12533.

(24) Zhang, Z.; Thung, Y. T.; Wang, L.; Chen, X.; Ding, L.; Fan, W.; Sun, H. Surface Depletion Effects in Bromide-Ligated Colloidal Cadmium Selenide Nanoplatelets: Toward Efficient Emission at High Temperature. *The Journal of Physical Chemistry Letters* **2021**, *12*, 9086–9093.

(25) Southworth, B. C.; Osteryoung, R.; Fleischer, K. D.; Nachod, F. C. The Polarography of Quaternary Ammonium Compounds. **2002**,

(26) Ashokan, A.; Mulvaney, P. Spectroelectrochemistry of Colloidal CdSe Quantum Dots. *Chemistry of Materials* **2021**, *33*, 1353–1362.

(27) Wang, L.; Xiang, D.; Gao, K.; Wang, J.; Wu, K. Colloidal n-Doped CdSe and CdSe/ZnS Nanoplatelets. *The Journal of Physical Chemistry Letters* **2021**, *12*, 11259–11266.

(28) Vong, A. F.; Irgen-Gioro, S.; Wu, Y.; Weiss, E. A. Origin of Low Temperature Trion Emission in CdSe Nanoplatelets. *Nano Letters* **2021**, *21*, 10040–10046.

(29) Carrillo-Carrión, C.; Cárdenas, S.; Simonet, B. M.; Valcárcel, M. Quantum dots luminescence enhancement due to illumination with UV/Vis light. *Chemical Communications* **2009**, 5214–5226.

(30) Jones, M.; Nedeljkovic, J.; Ellingson, R. J.; Nozik, A. J.; Rumbles, G. Photoenhancement of luminescence in colloidal CdSe quantum dot solutions. *The Journal of Physical Chemistry B* **2003**, *107*, 11346–11352.

(31) Gooding, A. K.; Gómez, D. E.; Mulvaney, P. The effects of electron and hole injection on the photoluminescence of CdSe/CdS/ZnS nanocrystal monolayers. *ACS nano* **2008**, *2*, 669–676.

(32) Zeng, Y.; Kelley, D. F. Excited Hole Photochemistry of CdSe/CdS Quantum Dots. *The Journal of Physical Chemistry C* **2016**, *120*, 17853–17862.

(33) Shulenberger, K. E.; Keller, H. R.; Pellows, L. M.; Brown, N. L.; Dukovic, G. Photocharging of Colloidal CdS Nanocrystals. *The Journal of Physical Chemistry C* **2021**, *125*, 22650–22659.

(34) Grimaldi, G.; Geuchies, J. J.; van der Stam, W.; du Fossé, I.; Brynjarsson, B.; Kirkwood, N.; Kinge, S.; Siebbeles, L. D. A.; Houtepen, A. J. Spectroscopic Evidence for the Contribution of Holes to the Bleach of Cd-Chalcogenide Quantum Dots. *Nano Letters* **2019**, *19*, 3002–3010.

(35) Taheri, M. M.; Elbert, K. C.; Yang, S.; Diroll, B. T.; Park, J.; Murray, C. B.; Baxter, J. B. Distinguishing Electron and Hole Dynamics in Functionalized CdSe/CdS Core/Shell Quantum Dots Using Complementary Ultrafast Spectroscopies and Kinetic Modeling. *The Journal of Physical Chemistry C* **2021**, *125*, 31–41.

(36) Jha, P. P.; Guyot-Sionnest, P. Trion Decay in Colloidal Quantum Dots. *ACS Nano* **2009**, *3*, 1011–1015.

(37) Kheng, K.; Cox, R. T.; d' Aubigné, M. Y.; Bassani, F.; Saminadayar, K.; Tatarenko, S. Observation of negatively charged excitons X- in semiconductor quantum wells. *Physical Review Letters* **1993**, *71*, 1752–1755.

(38) Kheng, K.; Cox, R. T.; d'Aubigné, Y. M.; Mamor, M.; Magnea, N.; Mariette, H.; Saminadayar, K.; Tatarenko, S. Negatively charged excitons X in the electron gas in CdTe/Cd1xZnxTe quantum wells. *Surface Science* **1994**, *305*, 225–229.

(39) Kossacki, P. Optical studies of charged excitons in II-VI semiconductor quantum wells. *Journal of Physics: Condensed Matter* **2003**, *15*, R471–R493.

(40) Astakhov, G. V.; Yakovlev, D. R.; Kochereshko, V. P.; Ossau, W.; Nürnberger, J.; Faschinger, W.; Landwehr, G. Charged excitons in ZnSe-based quantum wells. *Physical Review B* **1999**, *60*, R8485.

(41) Shornikova, E. V.; Yakovlev, D. R.; Biadala, L.; Crooker, S. A.; Belykh, V. V.; Kochiev, M. V.; Kuntzmann, A.; Nasilowski, M.; Dubertret, B.; Bayer, M. Negatively Charged Excitons in CdSe Nanoplatelets. *Nano Letters* **2020**, *20*, 1370–1377.

(42) Peng, L.; Otten, M.; Hazarika, A.; Coropceanu, I.; Cygorek, M.; Wiederrecht, G. P.; Hawrylak, P.; Talapin, D. V.; Ma, X. Bright trion emission from semiconductor nanoplatelets. *Physical Review Materials* **2020**, *4*, 056006.

(43) Antolinez, F. V.; Rabouw, F. T.; Rossinelli, A. A.; Cui, J.; Norris, D. J. Observation of Electron Shakeup in CdSe/CdS Core/Shell Nanoplatelets. *Nano Letters* **2019**, *19*, 8495–8502.

(44) Rossinelli, A. A.; Rojo, H.; Mule, A. S.; Aellen, M.; Cocina, A.; De Leo, E.; Schäublin, R.; Norris, D. J. Compositional Grading for Efficient and Narrowband Emission in CdSe-Based Core/Shell Nanoplatelets. *Chemistry of Materials* **2019**, *31*, 9567–9578.

(45) Bertrand, G. H. V.; Polovitsyn, A.; Christodoulou, S.; Khan, A. H.; Moreels, I. Shape control of zincblende CdSe nanoplatelets. *Chemical Communications* **2016**, *52*, 11975–11978.

(46) Boldt, K.; Kirkwood, N.; Beane, G. A.; Mulvaney, P. Synthesis of Highly Luminescent and Photo-Stable, Graded Shell CdSe/Cd x Zn1–x S Nanoparticles by In Situ Alloying. *Chemistry of Materials* **2013**, *25*, 4731–4738.

TOC Graphic

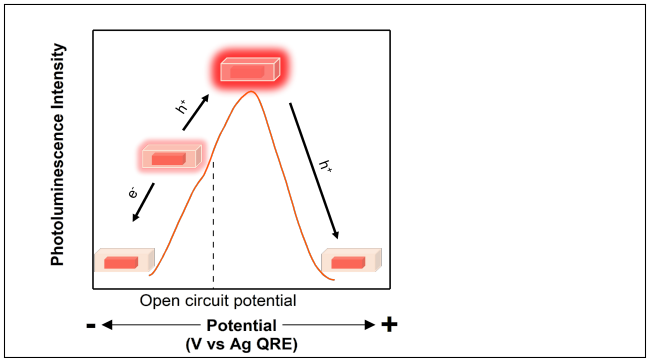
Photoluminescence Intensity
h+
e-
h+
Open circuit potential
-
Potential
(V vs Ag QRE)
+